

Structural and magnetic properties of nanometric Zn-ferrite prepared by different methods

K. BENKHOUSA^a, EL MOKHTAR LEMDEK^a, K. JAAFARI^a, M. BETTACH^b, M. TOUAIHER^a, K. SBIAAI^c, Y. BOUGHALEB^{c,d}, S. TOUHTOUH^{e,f}, A. HAJJAJI^f, REGINO-SAEZ-PUCHE^g

^aEMNED, Chemistry Department, Faculty of Sciences, UCD University, P.O. Box 20/24000, El Jadida, Morocco

^bLPCM, Chemistry Department, Faculty of Sciences, UCD University, El Jadida, Morocco

^cLPMC, Physics Department, Faculty of Sciences, UCD University, El Jadida, Morocco

^dHassan II Academy of Sciences and Technology, Rabat, Morocco

^eLMCPA, UVHC, F-59600 Maubeuge, France

^fENSA, National School of Applied Sciences, UCD, P.O. Box 1166 Plateau 24002, El Jadida, Morocco

^gDepartamento de Química Inorgánica I, Facultad de Ciencias Químicas, Universidad Complutense de Madrid, Ciudad Universitaria s/n, 28040 Madrid, Spain

This work has the objective of studying the influence of preparation methods on the structural, morphology and magnetic properties of ZnFe₂O₄ ferrites. The samples were prepared by various methods of synthesis (conventional ceramic method, sol-gel, freeze-drying and hydrothermal method), and were characterized by X-ray diffraction (XRD), (SEM) and (TEM) micrographs and magnetization measurements. The characteristics of ZnFe₂O₄ sample prepared by different methods have been studied to select the better method, i.e. the one that is the simplest and does not require an elaborate instrumental set-up. The results indicated that the hydrothermal method gives the lowest value for the lattice parameter (8.4261Å) and small nanosizes of particles (14 nm), while the highest values (a=8.4394Å and d=158.5 nm) are obtained with the ceramic method. The DC magnetization (2-300 K) measurements reveal a superparamagnetic behaviour for this sample prepared by hydrothermal method with a blocking temperature (T_B=12K). In the case the ceramic method T_B equal to 20K. Over the TB all the samples ZnFe₂O₄ show a paramagnetic behavior.

(Received April 17, 2013; accepted June 12, 2013)

Keywords: Nanometric Zn- ferrite, Spinel ferrites, Blocking temperature T_B, Superparamagnetism

1. Introduction

Spinel ferrites have been investigated since decades due to their potential applications in drug delivery, magnetic refrigeration, high density information storage, magnetic fluids, magnetic resonance imaging, etc. [1–6]. Zinc ferrite (ZnFe₂O₄) is known to be normal spinel structure with paramagnetic properties at room temperature and long range antiferromagnetic order below Néel temperature of about 10 K [7,8]. The paramagnetic properties of ZnFe₂O₄ come from the occurrence of negative superexchange interactions and Fe³⁺ on the octahedral sites [9–13]. In ZnFe₂O₄, Zn²⁺ cations occupy tetrahedral (A) and Fe³⁺ cations in octahedral (B) sites [14, 15].

It may be mentioned that this study of ZnFe₂O₄ represents an extension of other studies [16, 17]. There have been various reports demonstrating the feasibility of wet chemical preparation of the ZnFe₂O₄ nanoparticles via different approaches such as co-precipitation [18], sol-gel [19], aerogel [20], hydrothermal [21], solvothermal [22], by tartrate precursor method [23] or decomposition of organometallic compounds [24–27]. These processes attempt to yield finer-size powders by a more intimate mixing the starting materials. The molecular precursor approach offers the advantage of achieving an intimate

molecular-level mixing of the metal ions in the precursor. In our work, the ZnFe₂O₄ phases have been prepared by the classical ceramic method which yields sintered particles and it is not possible to obtain nanoparticles. For this reason, besides the conventional ceramic method, many other synthesis wet routes yielding nanosized samples of these materials have been reported, including sol-gel, freeze-drying and hydrothermal methods. In this work, the synthesis of the phases and the influence of the different methods on structural and on magnetic properties of the final ZnFe₂O₄ products are identified and discussed.

2. Experimental

2.1 Synthesis of ZnFe₂O₄

The zinc ferrite was prepared using different methods of synthesis: standard ceramic, sol-gel, freeze-drying and the hydrothermal technique. Some work has used a combination of coprecipitation and mechanical milling for cobalt ferrite [28]. Another study has compared the ceramic and sol-gel methods for nickel ferrite [29], while in the present paper we compare four different methods:

(1) Standard ceramic technique: stoichiometric amounts of Zn(NO₃)₂·6H₂O (4.15 mmol) and Fe(NO₃)₃·9H₂O (8.29 mmol) were placed in a crucible

and treated at 200 °C for 8h in air to decompose the nitrates. The mixture was heated at 800°C for 8h and finally at 900°C for 8h in air.

(2) Sol-gel: This is known as a technique for the low temperature synthesis of glass, ceramics and others. In this method, the raw materials, $\text{Zn}(\text{NO}_3)_2 \cdot 6\text{H}_2\text{O}$ and $\text{Fe}(\text{NO}_3)_3 \cdot 9\text{H}_2\text{O}$, were first dissolved in ethanol (26.02 ml), de-ionized water (50 ml), and finally tetraethoxyorthosilicate TEOS (Merk 98%) (6.50 ml) was added as a chelating agent under stirring until a homogeneous mixture was observed. In this stage of preparation, we note that the molar ratio of ferrite/ silica was 30:70. The mixture was heated at 60 °C for 3 days. The resulting gel was dried at 80 °C for 24 h and subsequently reheated at 600 °C for 2h, at 800 °C for 2h and finally at 900°C for 8h.

(3) Freeze-drying: stoichiometric amounts of $\text{Zn}(\text{NO}_3)_2 \cdot 6\text{H}_2\text{O}$ (4.15 mmol) and $\text{Fe}(\text{NO}_3)_3 \cdot 9\text{H}_2\text{O}$ (8.29 mmol) were dissolved in 80 ml of distilled water, under stirring until a homogeneous orange-brown dissolution was observed. The dissolution obtained was drop-by-drop frozen under liquid nitrogen and subjected to the freeze-drying process for 24h in a Telstar Laboratory Freeze-Dryer Cryodos-80 to remove water by sublimation at $T = -58$ °C. The powder obtained was calcined six times, at 400, 500, 600, 700, 750 and 770 °C. Under air atmosphere during 12h.

(4) Hydrothermal method: the ZnFe_2O_4 nanoparticles were prepared by this method in which stoichiometric amounts of iron and zinc nitrates were dissolved in distilled water obtaining a yellow solution. By adding a KOH 2M solution until pH = 11 using a pipette, the iron and zinc hydroxides were precipitated. This precipitate was transferred into a Teflon stainless-steel autoclave and heated for different periods of time, ranging from 3 hours to 15 hours at 160 °C to obtain Zn-ferrite. The final product was filtered and washed with distilled water and ground after drying in air.

The samples obtained by different methods were slowly cooled and between each heat treatment, the powder was ground using an agate mortar.

The flow chart of the synthesis route of each method is shown in figure 1.

2.2 Characterization

The structural phases of the samples were identified by X-ray powder diffraction employing a Siemens/ D-5000 X-ray diffractometer over a 2θ range from 20° to 70° using $\text{Cu } \alpha$ radiation ($\lambda = 1.5481$ Å). Microstructural characterization was evaluated by transmission electron microscopy (TEM) using a JEOL-2000FX electron microscope working at 200 kV. Scanning electron micrographs (SEM) were taken in a JEOL 6400 electron microscope working at 20 kV. Magnetic susceptibility and magnetization measurements were done in a Quantum Design XL-SQUID magnetometer in the temperature range of 2-300 K at different magnetic fields up to 5 T. Magnetic susceptibility measurements were performed after the sample was cooled at 2K in zero field cooling

(ZFC). In the so called field cooling measurements modality (FC) the sample was cooled in presence of the required magnetic field down to 2K.

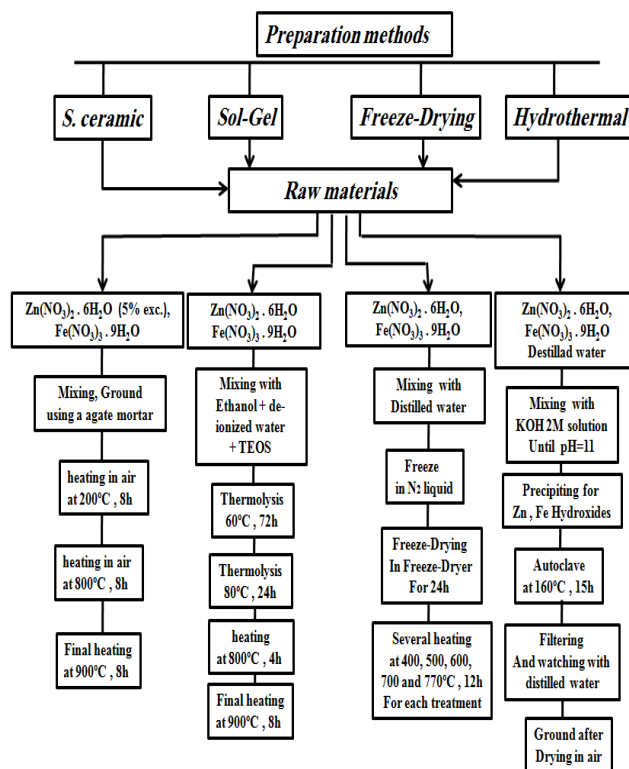


Fig. 1. Flow chart of different preparation routes.

3. Results and discussion

3.1 Crystalline structure

The XRD patterns of ZnFe_2O_4 prepared by four different methods are illustrated in figure 2. All the peak positions of all samples match very well and the maximum intensity peak in all samples corresponds to (311) plane and no secondary peaks were observed. These X-ray diffraction data reveal that all the samples obtained for all methods crystallize in a single phase pure of ZnFe_2O_4 with the cubic spinel type structure and space group $\text{Fd}\bar{3}\text{m}$. The sample prepared by the hydrothermal method has the lowest lattice parameter (8.4261 Å), while the largest value (8.4394 Å) was obtained with the standard ceramic method. The lattice parameter (a) as a function of the particle size for various preparation methods is shown in figure 3, and reported in table 1. It can be seen as well the evolution of the unit cell parameter of the samples prepared by various method with different particle size and it is found that this lattice parameter decreases with decreasing of the particle size of ZnFe_2O_4 prepared by different methods i.e. this parameter of the cell varies in

proportion to the choice of the preparation method of $ZnFe_2O_4$.

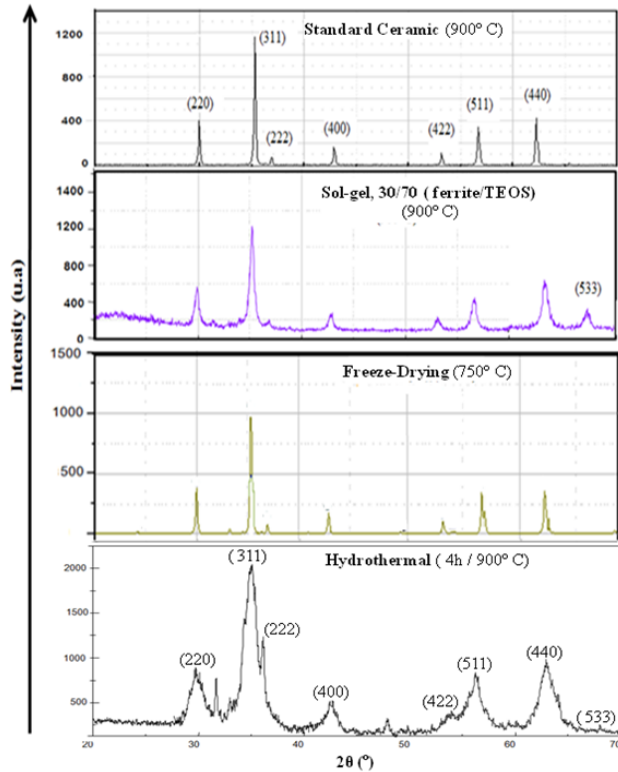


Fig. 2. XRD patterns of $ZnFe_2O_4$ prepared by different methods.

In other words, the lattice parameter is correlated with the particle size through increasing the d-spacing and decreasing $\cos\theta$.

Table 1. Synthesis conditions, results from XDR, crystallite size d , lattice parameter a and Blocking Temperature (T_B). ¹Calculated from TEM micrograph, ²Calculated from Scherrer formula

Synthesis method	$d^{(1)}$ (nm)	$d^{(2)}$ (nm)	a (Å)	T_B (K)
Ceramic	100 ~ 160	158.5	8.4394	20
Sol-Gel	60 ~ 90	75	8.4391	18
Lyofilisation	40 ~ 70	56.4	8.4283	15
hydrothermal	10 ~ 40	14	8.4261	12

The average particle size has been calculated using the well-known Scherrer's formula ($d = 0.9 \lambda / \beta \cos\theta$), where d is the crystalline size, λ the wavelength (Cu $K\alpha$), θ the Bragg angle and β the full width to half maximum of the (311) reflection on the $ZnFe_2O_4$ cell. The results indicated that the hydrothermal method give the smallest nanosize of particle (14 nm), while the highest values (158.5 nm) are obtained with the ceramic method (table 1).

The large full width at half maximum (FWHM) (of the order of degrees) deduced from the most intense diffraction peak confirms a very small value (of the order

of nanometers) of the diameter of ferrite nanocrystallites in the samples prepared by hydrothermal method.

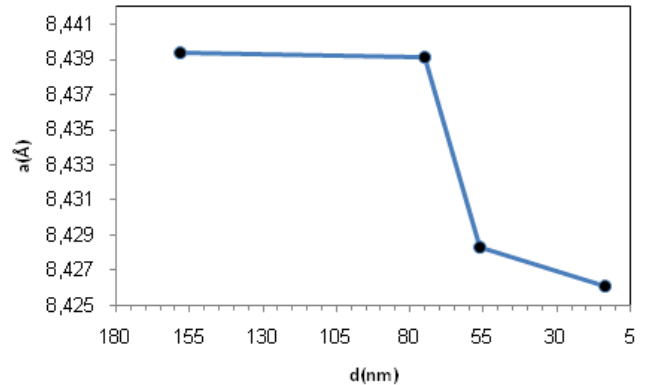


Fig.3. The lattice parameter a as a function of the particle size.

Thus, the TEM and SEM images of the $ZnFe_2O_4$ prepared by different methods are shown in figure 4. It is observed (table 1) that the prepared powder samples were in largest size (100 ~ 160 nm) for ceramic method and in nanosize with sizes less than 40 nm for hydrothermal (10 ~ 40 nm). Typical octahedral-shaped particles are visualized by TEM for the Zn-ferrite prepared by hydrothermal method. We observe a more homogenous particle size (figure 4d). The average size estimated from the image of about 60 particles of each sample was 14 nm.

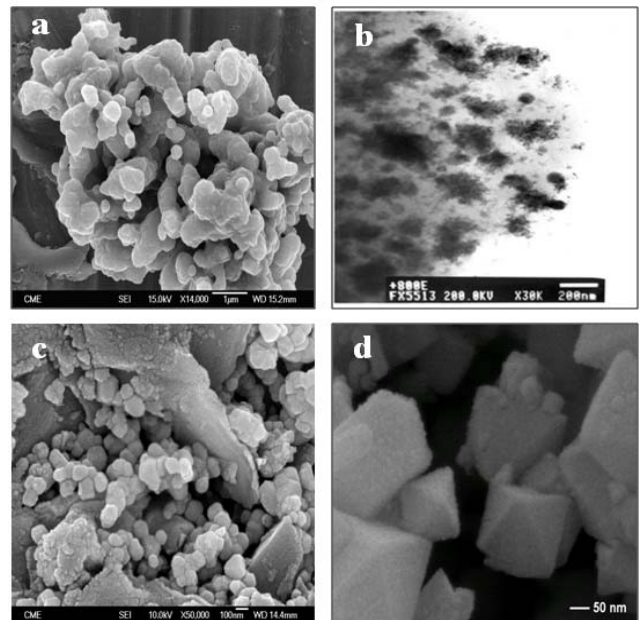


Fig. 4. SEM micrographs of $ZnFe_2O_4$ prepared by (^a Ceramic and ^c Freeze-Drying) methods and TEM micrographs of $ZnFe_2O_4$ prepared by (^b Sol-gel and ^d Hydrothermal) methods.

In this preparation method of Zn-ferrite, the particle size is in good agreement with the values obtained from the X-ray powder data, but the sample produced by the

ceramic method (figure 4a) is formed by bigger particles than those prepared by hydrothermal synthesis (figure 4d), also in the ceramic method the sample present a less homogenous particle size distributions.

The XRD of the prepared sample ZnFe_2O_4 seems to be different from one method to another, mainly due the difference in the crystal size of the obtained powder which varies from 158.5 nm in the ceramic method to 14 nm in the hydrothermal method. The variation of particle size of each method involves change in the lattice parameter as is clear in figure 3. Also, we can probably ascribe the difference in the XRD to the particle shape and distribution. It is clear that at larger particle size (figures 4-a, 4-b, 4-c and 4-d), the multidomain (MD) structure starts to predominate, after which the samples with a particle

size of 75 nm (sol-gel) and 158.5 nm (ceramic) are obviously completely MD.

3.2 Magnetic properties

Fig. 5-a, 5-b, 5-c and 5-d shows the temperature dependence of magnetic susceptibility in the ZFC and FC processes with an applied field $H = 500$ Oe for the ZnFe_2O_4 spinel prepared by different methods. The values of χ decrease with increasing temperature, which is the trend for spinel ferrimagnets, until reaching the Curie point after which the sample behaves as paramagnetic. Also, the shape of the χ_{M-T} curve depends strongly of the particle size, i.e. of the method of preparation.

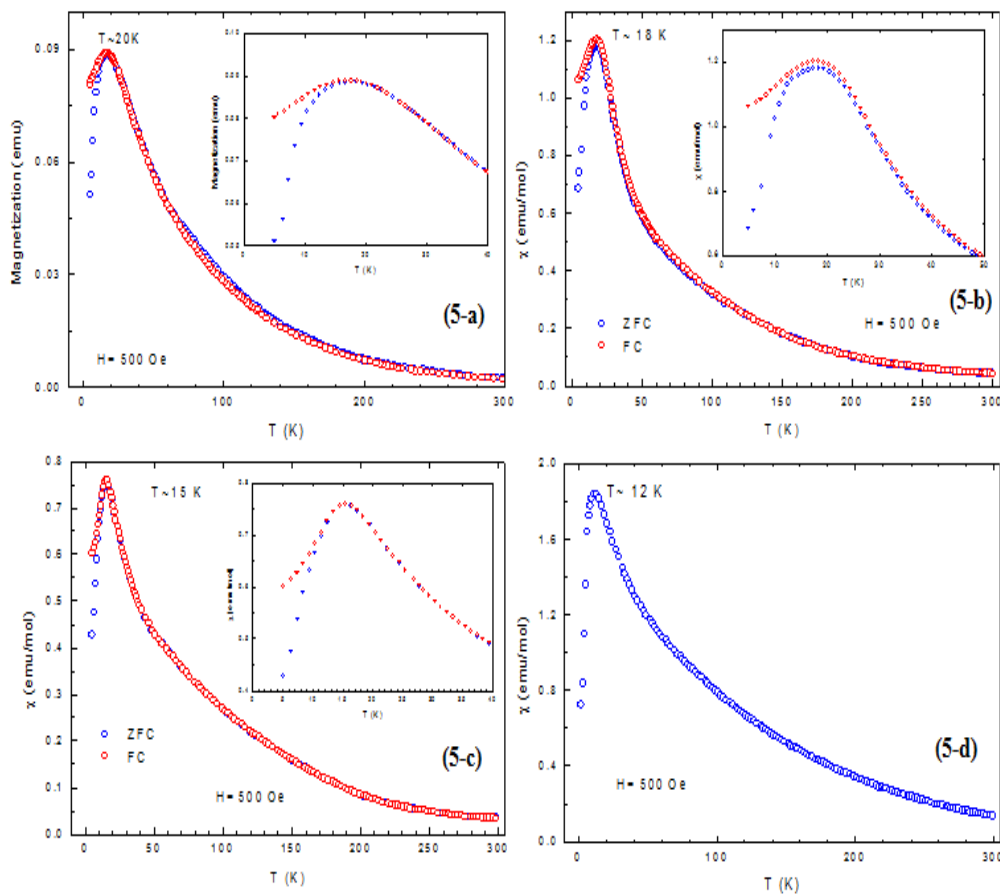


Fig. 5. The temperature dependence of molar magnetic susceptibility in the ZFC and FC for the ZnFe_2O_4 prepared by ceramic method (5-a), Sol-gel (5-b), Freeze-drying (5-c) and hydrothermal method (5-d).

It is clear from table 1 that the value of the Blocking temperature (T_B) change when the particle size vary. The sample prepared by the hydrothermal method has the lowest value blocking temperature ($T_B=12\text{K}$), while the largest value ($T_B=20\text{K}$), was obtained with the standard ceramic method. The sample prepared by the hydrothermal method has superparamagnetic behavior, where it is dominated by single domain particles (SD) rather than multidomain (MD). The general trend of χ_{M-T} for all samples prepared by other synthesis methods, except that prepared using the hydrothermal method, is nearly the

same, exhibiting the well known behavior of spinel ferrites obeying the Curie-Weiss law below T_B .

The maximum of χ_M agrees with the change in the spin canting in ZnFe_2O_4 observed by Mössbauer spectroscopy [30]. In addition to this broad anomaly, also the spin sample like blocking of magnetic moments around $T \sim 10$ K can be assigned to ZnFe_2O_4 . The concave shaped $\chi(T)$ curves indicate a low density and localized nature of the carriers in this sample [31].

However, below the blocking temperature, the particles do not have enough energy to reach the thermal

equilibrium and the hysteresis appears. The inverse susceptibility χ (magnetization) as a function of the

temperature for the ZnFe_2O_4 prepared by different methods shown in the figures 6-a, 6-b, 6-c and 6-d.

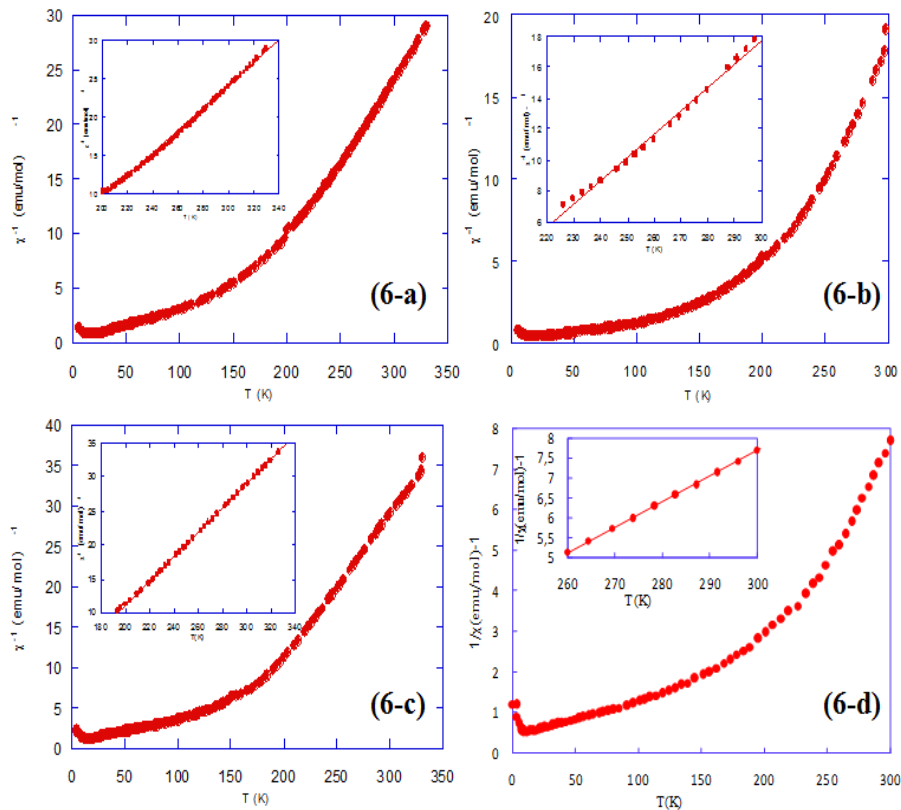


Fig. 6. The reciprocal molar magnetic susceptibility as a function of the temperature for the ZnFe_2O_4 prepared by ceramic method (6-a), Sol-gel (6-b), Freeze-drying (6-c) and hydrothermal method (6-d).

It reveals two regimes of the Curie-Weiss behavior of $\chi = C/(T-\theta)$ over a very narrow temperature range (260-300K) and a positive value of the Weiss temperature as high as 180K for sample prepared by hydrothermal method (figure 6d). The compound prepared by ceramic method has even behavior but in a wider temperature range (170-300K) and a small positive value of the Weiss temperature equal to 130K (figure 6a). This result combined with the values of the magnetization obtained at low temperatures (figure 5d) is consistent with the presence of a ferrimagnetic behaviour arising from the partially inverse character of this ZnFe_2O_4 spinel.

This behavior for sample prepared by hydrothermal method is confirmed from the magnetization curve obtained at 300 K (figure 7d) where the coercive field and remanence have a small value. This indicates that ZnFe_2O_4 nanoparticles synthesized by hydrothermal method behave as superparamagnetic at 300 K.

It has been known [32] that magnetic particles with a size smaller than a few tens of nanometers can be considered as single domains and, hence, displays properties markedly different from the bulk. One of the interesting features of nanosize magnetic materials is the presence of a magnetic relaxation process that is due to the thermal effect and the existence of energy barriers separating the local minima for different equilibrium states of the system.

As a result, the magnetic behavior of a small particle depends on its relaxation time (τ). When τ is smaller than the experimental time, the magnetization vector is seen to change quickly between different states, i.e. the system is in a superparamagnetic state. By contrast, when $\tau > \tau_{ex}$, the thermal dynamic equilibrium state is very difficult to observe, since the energy barriers arising from the anisotropy obstruct the magnetization vector from switching to a lower-energy state. This case is generally called the blocked state.

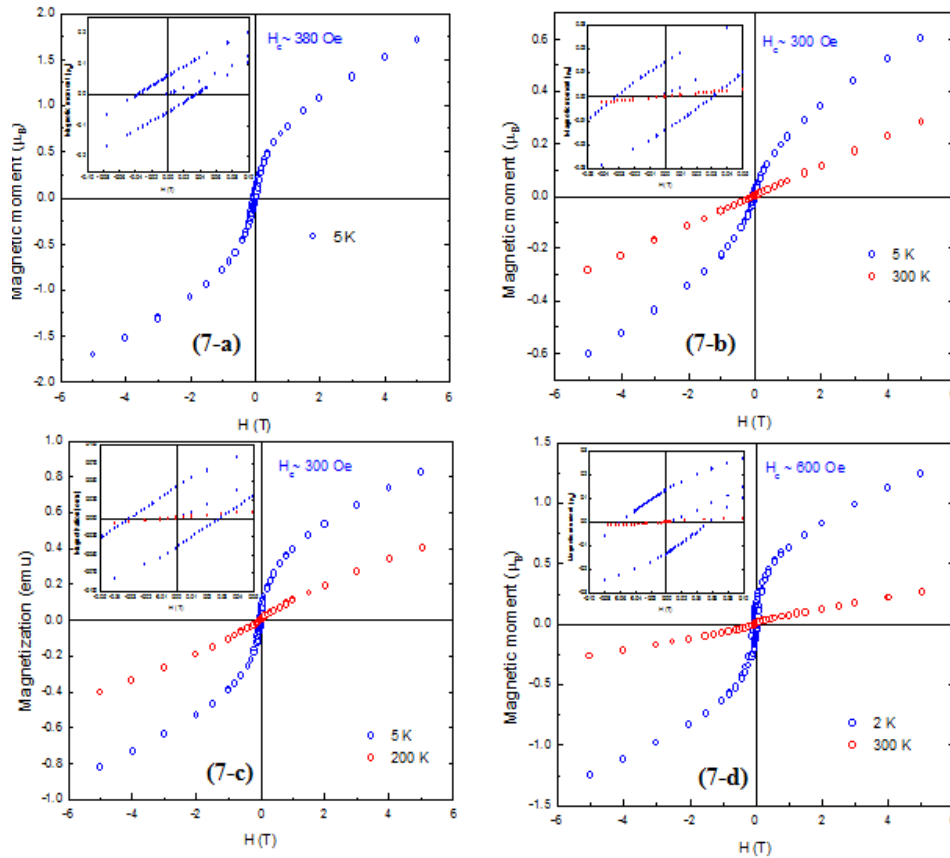


Fig. 7. The magnetization loop obtained at 5 K (blue) and 200 K or 300 K (red) for the ZnFe_2O_4 prepared by ceramic method (7-a), Sol-gel (7-b), Freeze-drying (7-c) and hydrothermal method (7-d).

The temperature at which $\tau = \tau_{\text{ex}}$ is defined as the blocking temperature. This will be studied in future work. Another interesting feature of the nanoparticles is due to the surface spin disorder which is induced by the broken exchange bonds at the surface. This is especially true for the case of ferrites, where the negative superexchange interaction is mediated by an intervening oxygen ion, and it can be missing at the surface.

As a result, the system should be considered as a core-shell structure with ferromagnetically aligned core spins and a spin-glass like surface layer. It is observed that domain wall motion was absent in SD particles [33]. Also, it is suggested that the domain wall motion is increased by increasing the particle size [34]. These variations were attributed to the change in domain configuration with particle size.

From a closer look at the data in table 1, we can find similar trends to those reported earlier [33–36] for the samples prepared by the sol-gel and standard ceramic techniques where the MD structure dominates and the magnetic behavior is attributed to the negative exchange interaction resulting from antiferromagnetic coupling between magnetic ions on A and B sites.

Finally, the present study shows that the properties such as Blocking temperature and particle size of Zn-ferrites processed by the hydrothermal method are comparable to, and in some cases even better than, those reported for ferrites prepared by the ceramic method and

some other wet methods. The sintering temperatures and durations are relatively lower in the precursor method. The hydrothermal method is capable to give smaller grains than the ceramic method and it is possible to obtain a wider range of properties.

4. Conclusions

The ZnFe_2O_4 oxide has been prepared by various methods as a single phase with cubic structure belonging to the fcc system. The wet chemical methods are gaining prominence for the preparation of homogeneous and compositionally stoichiometric ferrites. The particle size, lattice parameter and blocking temperature depend on the nature of preparation methods.

The value of lattice parameter is highest in the ceramic method while this value decreases in all the wet methods depending on the particle size and the melting point of the raw materials.

The hydrothermal method we suggest is better than the other methods and allows obtaining a very fine nanoparticle dimensions (average size of 14 nm) and more homogenous size. The small and homogenous obtained by hydrothermal method lead to a perfectly superparamagnetic behavior with blocking temperature of 12 K and a lowest lattice parameter (8.4261 Å).

We conclude that the physical properties of the ferrite according to the required application are parametric by choosing a suitable method of preparation with low cost and optimum characterization.

Acknowledgements

Thanks are due to Spanish MEC for financial support under Research Project MAT2003-08645-C01-02 and to the AECI Project 193/03/P. The contributions of several researchers at the Departamento de Quimica Inorganica I, (Universidad Complutense, Madrid, Spain) and (Universidad Polytechnica, Madrid, Spain), are most gratefully acknowledged.

References

- [1] L. Gama, A. P. Diniz, A. C. F. M. Costa, S.M. Rezende, A. Azevedo, D. R. Cornejo. *J. Magn. Magn. Mater* **384**, 97(2006).
- [2] G.C. Lin, Q, J. X. Wei Zhang. *J. Magn. Magn. Mater* **300**, 392(2006).
- [3] A. R. Dinesen, S. Linderoth, S. Morup. *J. Phys. Condens. Mater* **17**, 6257(2005).
- [4] Y. Xu, A. M. Meier, P. Das, M. R. Koblischka, U. Hartmann. *Crystal. Eng* **5**, 383 (2002).
- [5] Y. S. Koo, D. H. Kim, J. H. Jung. *J. Korean. Phys. Soc* **48**, 677(2006).
- [6] S. I. Park, K. R. Choi, T.J. Kouh, C. S. Kim. *J. Magnetism* **12**,137(2007).
- [7] T. Sato, K. Haneda, M. Seki, T. Iijima. *Appl. Phys. A. Solids. Surf* **50**, 13(1990).
- [8] M. Sultan, R. Singh. *J. Appl. Phys* **105**, 07A512(2009).
- [9] D. Guo, J. Zhu, Y. Yang, X. Fan, G. Chai, W. Sui, et al. *J. Appl. Phys* **107**, 043903(2010).
- [10] C. Upadhyay, H. C. Verma, V. Sathe, A. V. Pimpale. *J. Magn. Magn. Mater* **312**, 271(2007).
- [11] M. K Roy, B. Haldar, H. C. Verma. *Nanotechnology* **17**, 232 (2006).
- [12] E. J. Choi, Y. Ahn, E. J. Hahn. *J. Korean. Phys. Soc* **53**, 2090 (2008).
- [13] S. Nakashima, K. Fujita, K. Tanaka, K. Hirao. *J. Phys. Condens. Matter* **17**, 137 (2005).
- [14] J. Smith, H. P. J. Wijn. *Ferrites Physical Properties of Ferrimagnetic Oxides in Relation to Their Technical Applications*. Eindhoven: Phillips (1959).
- [15] A. Goldman. *Modern Ferrite Technology*. Second Edition. U.S.A.: Springer (2006).
- [16] Y. F. Chen, D. Spoddig, M. D. Ziese. *J. Phys. Appl. Phys* **41**, 205004 (2008).
- [17] M. Bohra, S. Prasad, N. Kumar, D. S. Misra, S. C. Sahoo, N. Venkataramani, et al. *Appl. Phys. Lett* **88**, 262506(2006).
- [18] S. Nakashima, K. Fujita, K. Tanaka, K. Hirao, T. Yamamoto, I. Tanaka. *J. Magn. Magn. Mater* **310**, 2543(2007).
- [19] N. Wakiya, K. Muraoka, T. Kadowaki, T. Kiguchi, N. Mizutani, H. Suzuki, et al. *J. Magn. Mater* **310**, 2546(2007).
- [20] H.H. Hamdeh, J.C. Ho, S.A. Oliver, R.G. Willey, G. Oliveri, G. Busca. *J. Appl. Phys.* **81**(851), 1857(1997).
- [21] X. Jiao, D. Chen, Y. Hu. *Mater. Res. Bull.* **37**, 1583(2002).
- [22] V. B. Gutierrez, E. C. Pascual, M. J. T. Fernandez, *J. Solid State Chem* **184**, 1608 (2011).
- [23] J. M. Yang, F. S. Yen, *J. Alloys and Compounds* **450**, 387 (2008).
- [24] V. Moye, K.S. Rane, V.N.K. Dala, *J. Mater. Sci. Elect.* **1**, 212 (1990).
- [25] J. M. Yang, W. J. Tsuo, F.S. Yen, *J. Solid State Chem.* **160**, 100 (2001).
- [26] P. Ravindranathan, K. C. Patil, *Am. Ceram. Soc. Bull.* **66**, 688 (1987).
- [27] F. J. Guaita, H. Beltran, E. Cordocillo, J. B. Carda, P. Escribano, *J. Eur. Ceram. Soc.* **19**, 363 (1999).
- [28] R. H. Kodama, A. F. Berkowitz, E. F. M. Niff Jr. S.Foner, *Phys. Rev. Lett.* **77**, 394(1996).
- [29] J. A. March, M. L. Vicent, J. C. Paus, M. A. Gomez G. M. Tomas, *J. Solid. State.Sci* **26**, 91(2005).
- [30] S. A. Oliver, H. H. Hamdeh, and J. C. Ho, *Phys. Rev. B* **60**, 3400 (1999).
- [31] S. Das Sarma, E. Hwang, and A. Kaminski, *Phys. Rev. B* **67**, 155201(2003).
- [32] Z. X. Tang, C. M. Sorensen, K. J. Klabunde, *Phys. Rev. Lett* **67**, 3652(1991).
- [33] J. J. Shrotti, S. D. Kulrkarni, C. E. Deshpande, *J. Mater Chem. Phys* **59**, 1(1991).
- [34] S. Yan, J. Geng, L. Yin, E. Zhou, *J. Magn. Magn. Mater.* **277**, 84 (2004).
- [35] Y. Ahn, E. J. Choi, E. H. Kim, *Rev. Adv. Mater. Sci.* **5**, 477 (2003).
- [36] X. Li, C. Kotal. *J. Alloys. Compounds.* **394**, 264(2003).

*Corresponding authors: khalilbenkhouja@gmail.com